LABORATORI NAZIONALI DI FRASCATI
SIS-Pubblicazioni

LNF - 04 / 6(IR)
24 Marzo 2004

PROGETTO E REALIZZAZIONE DI UN MANIPOLATORE MICROMETRICO A SEI GRADI DI LIBERTÀ PER SPETTROSCOPIA A BASSA TEMPERATURA IN ALTO VUOTO

PROJECT AND MANUFACTURING OF A HIGH-VACUUM, SIX-AXES MICROMANIPULATOR FOR LOW TEMPERATURE SPECTROSCOPY

A. Marcelli[1], G. Cibin[2] and A. Raco[1]
[1)] *INFN, Laboratori Nazionali di Frascati, P.O. Box 13, I-00044 Frascati, Italy*
[2)] *INRM, P.za dei Caprettari,70 I-00186 Roma, Italy*

Abstract

Nell'ambito del progetto *CryoAlp* è stato sviluppato e collaudato un sistema di movimentazione micrometrica a sei gradi di libertà progettato per esperimenti di microscopia e spettroscopia in alto vuoto. Le caratteristiche di questo sistema micrometrico, dimensioni compatte, ampio campo operativo unito ad alta precisione, possibilità di eseguire mappature di superfici con geometrie complesse, compatibilità con ambiente di alto vuoto, temperature di esercizio fino a -50 ^{o}C, rendono questo sistema unico nel suo genere per esperimenti non convenzionali su campioni con superfici irregolari, in condizioni di temperatura controllata in vuoto.

In the framework of the *CryoAlp* project we developed and tested a micro-positioning system with six degrees of freedom devoted to spectromicroscopy experiments in a high-vacuum regime. The characteristics of this micrometric system: compactness, wide operating range combined to a high precision, capability to perform mapping of sample surfaces with complex geometries, compatibility with high-vacuum, operating temperatures down to -50 ^{o}C - make this system a unique system, tailored to specific requirements of non conventional experiments, such as those looking at samples with non homogeneous surfaces, in a controlled temperature regime in vacuum.

PACS: 07.85.Qe, 92

1 Introduction

Nowadays synchrotron radiation is the most brilliant source available in order to characterize materials having complex chemical composition and structure. In the last decade the impressive brilliance capability offered by third generation synchrotron sources existing all around the world make possible experiments with spectroscopic techniques in many case unimaginable using conventional sources. Actually, the use of synchrotron radiation sources exploits its best advantage when information coming from samples having extremely high dilutions are needed (e.g., the photon flux intensity is the most important parameter for the experiment) or in spectro-microscopy experiments where the beam illuminates an area of a few microns (e.g., the brilliance is the crucial parameter). In the latter situation, the availability of a micrometric system, compatible with particular experimental environments, is a challenging task. The major difficulties arise from the need of a high precision positioning in a high vacuum environment, with a number of degrees of freedom high enough to match needs of complex surface mapping procedures. We will describe in the next the characteristics of a new micrometric manipulation device, realized in the framework of a project devoted to the construction of a flexible microanalysis experimental system. This device was born to be used with intense and brilliant synchrotron radiation sources, but it can be certainly used with a lot of advantages with standard or conventional light sources. This work was triggered by the spectroscopical researches promoted within the framework of the *CryoAlp* project recently funded by INRM [1], the Italian Institute for Scientific and Technologic Research on Mountain environment. This project appears as a meeting point among different technical and scientific interdisciplinary expertise all together looking at the science of the alpine cryosphere, i.e., the natural environment of the Italian high mountains, with the common objective of the coordination and advancement of the scientific knowledge of the high mountain environment. Within the *CryoAlp* project we proposed several spectroscopic experiments to be performed on natural polycristalline ice materials characteristic of such an environment, like the ones obtained by deep hole sampling in glaciers or frozen soil - permafrost on microscopy scale. This is obviously due to the importance, on a natural environment at large scale, of the microscopic chemical and structural characteristics of these non-homogeneous aggregates under investigation. Among the many applications of this powerful experimental approach, we have to underline the possibility to investigate in a non-destructive way, the structure of ice samples taken at different depths of alpine glaciers, with important implications to the glaciology understanding (motion, time evolution and structure of the Italian glaciers), to measure the presence of trace element impurities [3], to obtain informations on the history of polluting substances deposition on the high mountains [4],

on the mineralogical characterization of fine powders found in ice [2] and transported by high altitude atmospheric circulation currents, or the study of permafrost, the frozen soil found in the highest parts of the alpine arc which plays a key role in the hydrogeological cycle dynamics [6].

2 Characteristics of the micrometric apparatus

The technical requirements of an apparatus dedicated to microscopy and spectroscopy experiments using synchrotron radiation in the X-ray and IR spectral regions are well defined and, in particular, a high vacuum experimental chamber is necessary. Moreover, in our research, the samples under investigation, e.g., ice or frozen water, require also cryogenic temperatures and, because the samples are natural systems containing trace impurities, the experimental environment has to be kept as clean as possible to prevent ambient contamination during all steps of the experiment to guarantee reliable detection of very low concentrations of pollutants.
Having these constraints in mind, we designed an integrated device based on a vacuum-compatible micropositioning system including detectors and a cryogenic cooler, all contained in a quite small and multi-purpose experimental chamber. The heart of the instrumentation is the manipulator, a prototype that is the result of the profitable interaction with the MICOS Gmbh Company, which at the end manufactured the first SpaceFab device characterized in this technical note. Its almost unique design and main characteristics allow a sample stage translation movement in 3D and rotation movements around three axes. Using the SpaceFab proprietary software the operator has complete freedom in the choice of the motion trajectories, to scan complex surfaces with micrometric precision in a working region some cm large, however with an angular precision of the order of magnitude of microradians in any direction. The SpaceFab is the first instrument of such kind fully compatible with high vacuum operations, optimized in size to match a vacuum chamber with NW400 flanges. These characteristics, together with the possibility of operating at low temperatures (down to -50 ^{o}C) without loss of performance, but for a lower speed, make this device really a unique sample holder.

The manipulator is controlled via Ethernet by TCP/IP protocol, or serial port (RS232). The system may control independent or combined movements of any of the six manipulator axes. The motion is completely programmable, maintaining the maximum freedom of choice in the motion directions. Actually, it is possible to the operator to program any trajectory for the sample stage, including a curved path or a motion on a curved surface, while leaving a constraint such as a point, a straight line or plane, unaltered during the motion.

Table 1: Main technical data of the MICOS SpaceFab^{TM}

Independent axes	6
Movement controls	X, Y, Z, θ, ϕ, ψ
Motion range	+/- 2.5 cm (X,Z) +/- 1.25 cm (Y)
	+/- 5^o (θ, ϕ, ψ)
Tolerances	+/- 10 μm (X,Y,Z)
	+/- 10 μrad (θ, ϕ, ψ)
Min. operating pressure	10^{-7} mbar
Operating temperature range	-50 / +80 ^{o}C
Max. load	1 Kg

3 Characterization of the SpaceFab^{TM}MICOS

To characterize the SpaceFab^{TM}we performed a series of tests to carefully evaluate its positioning accuracy and movement reproducibility in air. The main goal of the tests was the determination of the maximum difference between the required and achieved position, for any directions and rotations. The position measurements have been performed using a laser interferometric system (JENAer Metechnik ZLM), and were performed in air at room temperature. The results of the tests guarantee about the requirements of the realized instrumentation according to the project specifications. In addition, we verified full operational capability at low temperature and this achievement is certainly the most important condition to investigate natural and synthetic ice (see 3.1). The test set has been summarized in Table 2 while a detailed description of the measurements is reported in the Appendix.

3.1 Tests at low temperature

Some of the tests of Table 2 have been also performed at low temperature, by cooling down to a temperature of -50 ^{o}C the whole manipulator inside a temperature-controlled chamber. The measured performances confirmed the complete functionality of the system also under such hard environmental conditions. However, when working at low temperature the maximum speed motion has to be reduced of about 50 %.

4 The high vacuum chamber

The micropositioner is installed in a stainless steel (AISI 316L) HV chamber designed and manufactured *ad hoc* by DG Technologies (Parma). We designed the experimen-

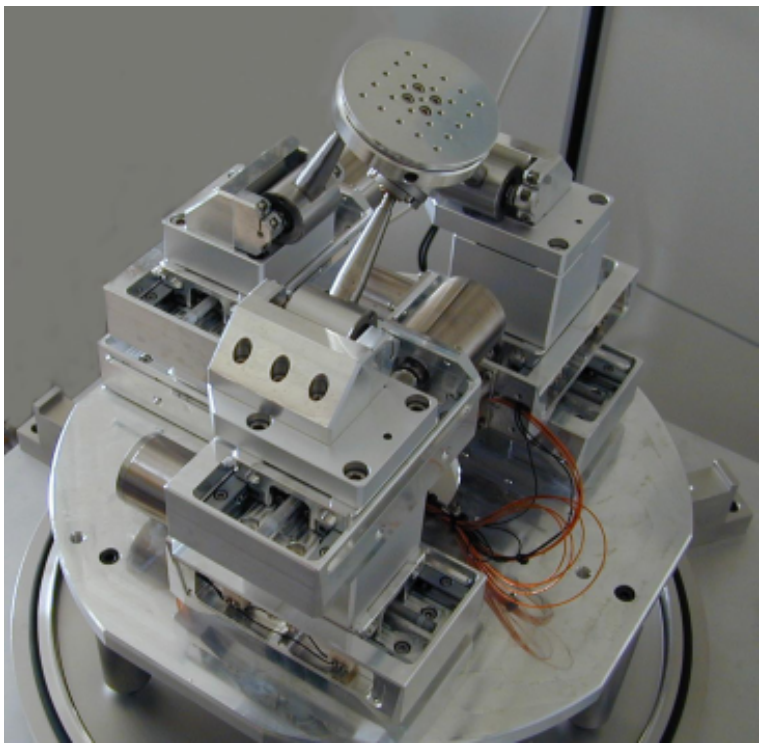

Figure 1: Picture of the MICOS SpaceFab manipulator.

tal chamber, taking in consideration the main experimental parameters (among them, the possibility to perform spectroscopies in extreme conditions) and both limited size and maximum flexibility to guarantee an easy installation at different synchrotron radiation experimental facilities. Additional main specifics were: cryogenic setup compatibility, integration with the microscopic system positioning, choice of materials to minimize the potential contaminations of the investigated samples. In figures 4 and 5 we show respectively a schematic drawing and a picture of the HV chamber. Before to integrate the SpaceFab inside the HV chamber, this latter was vacuum tested without any preliminary baking procedure, achieving a vacuum limit of 10^{-6} mbar.

After the vacuum tests of the experimental chamber, the micromanipulator has been installed and motion tests have been also performed in vacuum. The results of these more complex measurements will be presented in a forthcoming note [6].

The HV chamber layout is compatible with the possibility to perform experiments in the X-ray region, using both X-ray fluorescence and electron detectors, and the installation of a photoelectron microscope (PEEM). The use of a PEEM detector [7] combined with the use of synchrotron radiation sources may allow challenging investigations on nano-

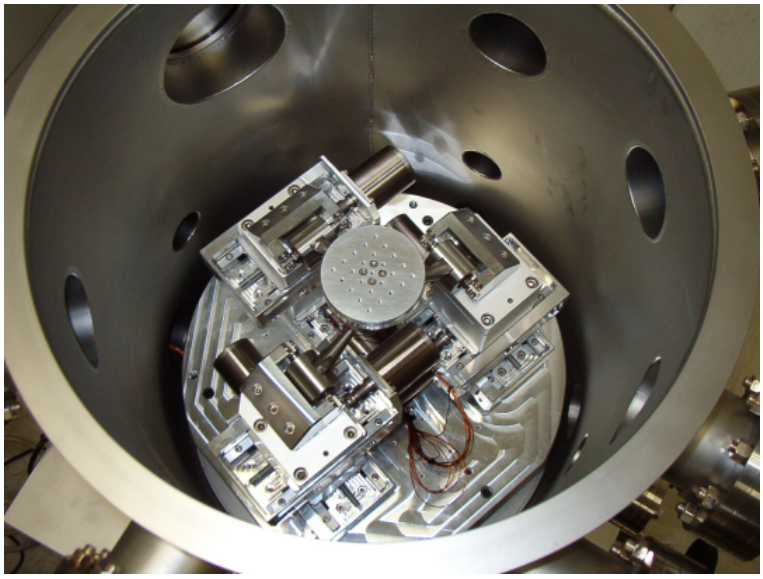

Figure 2: Manipulator installed in HV experimental chamber.

sized materials, e.g., the natural substances entrapped in an ice matrix, and probably the characterization of both composition and morphology with the highest spatial resolution available nowadays. The combined manipulator characteristics and chamber design allow to perform analysis and/or detection of trace element impurities not only during conventional experiments, such as ReflEXAFS and Total X-ray Reflection Fluorescence but also by new techniques based on inelastic scattering experiments (e.g., RIXS). In addition, also IR cryo-spectroscopy experiments have been planned and a study of the optical configurations to integrate the chamber with an existing Michelson interferometers for FTIR spectroscopy is in progress.

5 The cryogenic system for experiments on ice and frozen water

Because of the special need associated to the investigation of natural ice samples, we carefully evaluated many commercial cooling systems to select the most suitable for our experiments. Low temperature spectroscopical experiments demand for light, compact, vibration-free and vacuum compatible devices. In addition to the above requirements, one of our most challenging device requirement is the necessity to install it on the manipulator head, considering that the power and control connections have to not affect the motion capability of the system (see Table 1). The cryogenic system has to be also compatible with a simple load-lock sample system. In order to easily achieve very low temperatures

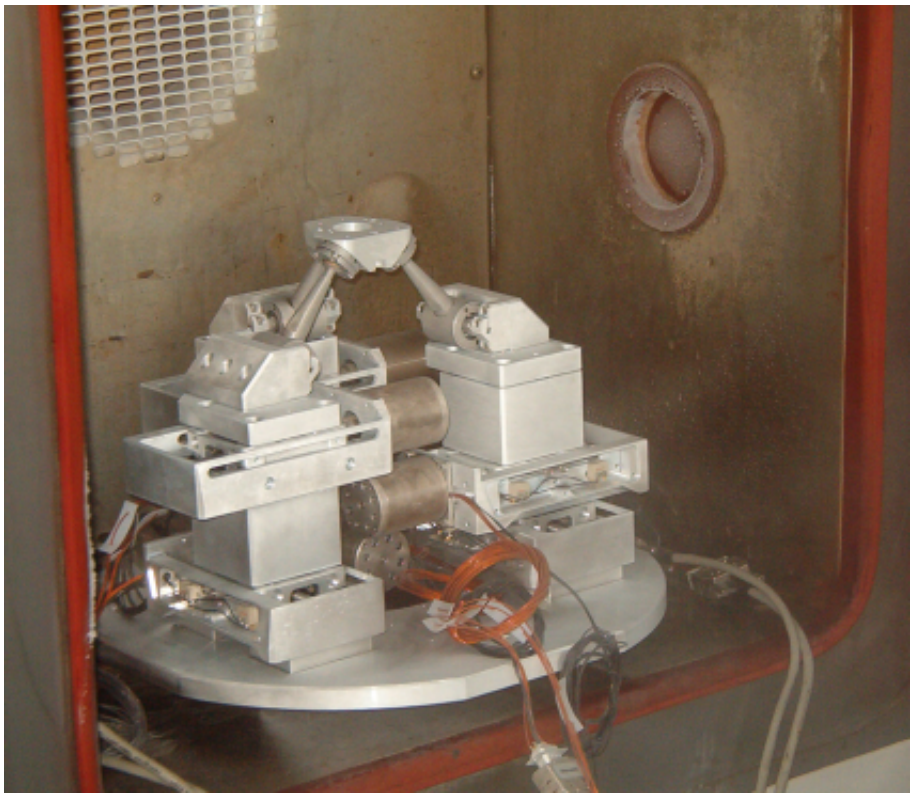

Figure 3: SpaceFab micromanipulator after the mechanical test at low-temperature. For such tests the manipulator was installed in a closed chamber cooled down to -50 ^{o}C.

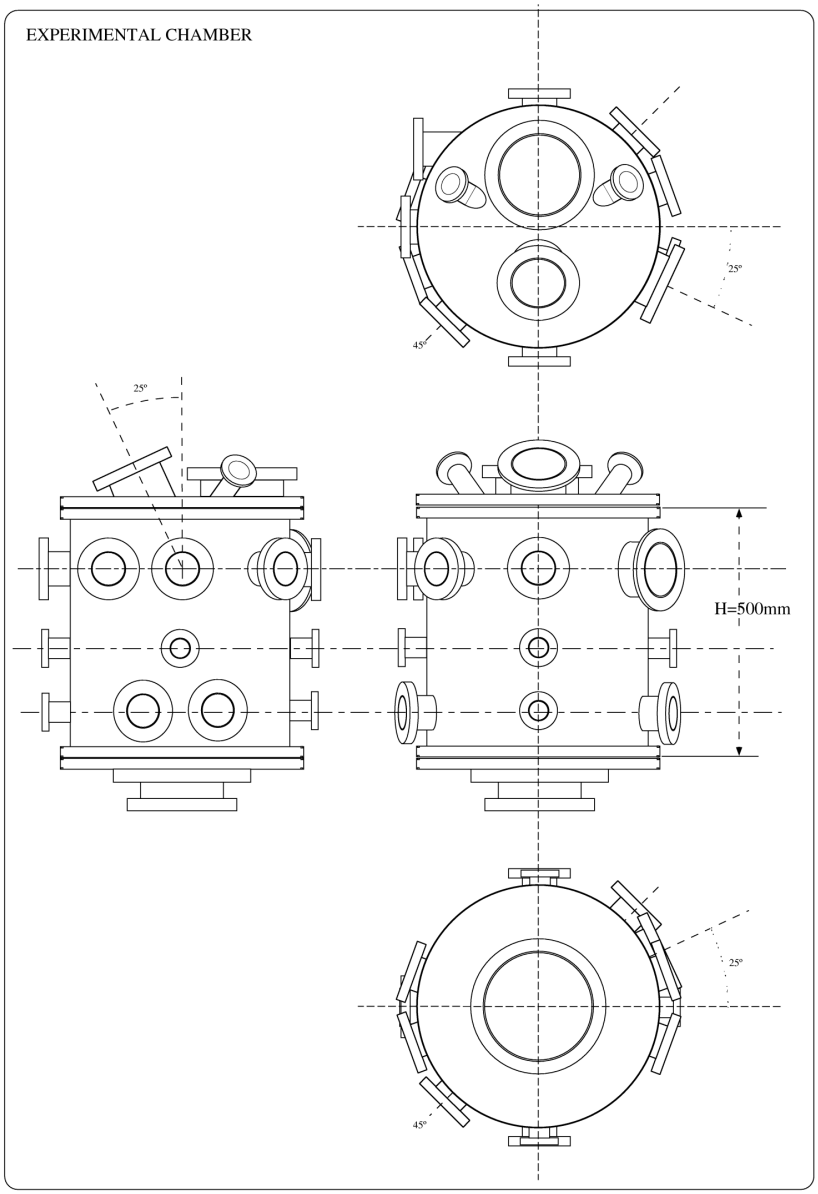

Figure 4: Schematic drawing of the HV experimental chamber.

Figure 5: The experimental chamber and its support during the preliminary vacuum tests at Frascati.

Table 2: Schematic results of the mechanical tests performed on the SpaceFab^{TM} using a laser interferometer JENAer Metechnik ZLM monitoring the sample stage position.

static stability average	20 nm, max. 80 nm (up to 1 minute)
accuracy for translations	10 μm (X,Z), 50 μm (Y), repeatability +/- 1 μm
accuracy for rotations	50 μrad
transverse displacement respect to any motion direction	$<$ 8 μm, +/- 2 μm
angular displacement during parallel translation motion	$<$800 μrad repeatability +/-100 μrad
repeatibility test for parallel translations	100 nm
repeatibility test for rotations	10 μrad
dynamic stability for translation	0.2 μm

(necessary in particular to investigate amorphous ices) we selected as the most suitable system a glass Thomson cooling system. This very light cryo-cooler developed by MMR Technologies (Mountain View, CA) may use high pressure gas lines compatible with HV requirements. This kind of cooling system allows a very fast temperature cycle control, and the possibility of reaching low temperatures (around 80 K for a compressed N_2 one-stage system, and down to 40$\sim$50 K in a particular two stages setup using compressed Ne). The main disadvantage associated to this system is the need for a high pressure flexible metal gas line in the vacuum chamber, that must guarantee the absence of gas leaks also after a high number of manipulator movement cycles. A high pressure gas source and flow control regulator system are also needed. Waiting for additional funding to complete with this instrumentation the existing apparatus, we developed a simple and very light cryogenic system, based on Peltier cells. These latter do not need any cryogenic fluid, they are extremely light and independent from cryogenic supplies. However the temperature range achievable is significantly limited (down to a minumum of -40 ^{o}C). Both the control and the power connections of Peltier cells can be made of extremely flexible electrical wires, so that this preliminary setup has been chosen because of its quite simple sample transfer line. Conversely, the major issue to face up with the use of a Peltier cell is the need of dissipating the excess of heat generated by the semiconductor system because of its low cooling efficiency. Several solutions have been considered and a first prototype has been recently tested with success. A double stage Peltier assembly for in-vacuum experiments, mounted onto a copper base and having independent temperature control over each cell cooling stage is indeed under test (see Figure 6) and will be used

for the first experiments on ice samples [8].

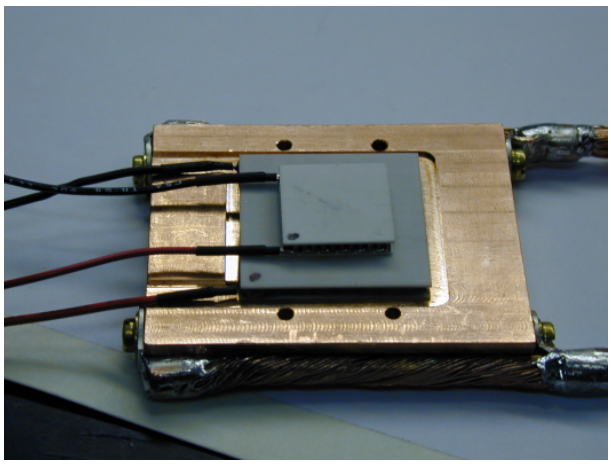

Figure 6: The double stage Peltier cell cryostat prototype under test.

6 Acknowledgments

We gratefully thank MICOS Gmbh and in particular Guido Giorgi (MICOS Italia) for his invaluable friendly technical support. A special thank is due to Emilio Burattini for his continuous support and for many useful advices and suggestions and to Antonio Grilli for his really unique technical support.

References

[1] S. Pignotti, *Il ruolo della criosfera alpina nel ciclo idrologico*, SLM n.7 (2003).

[2] G. Rossi, A. Novo, V. Maggi, G. Orombelli and C. Smiraglia, *Deep coring on the Lys glacier (Monte Rosa): First results*, Houille Blanche-Revue Internationale de l'Eau **53** (5-6), 124-127 (1998).

[3] I. Schwikowski, C. Barbante, T. Doering, H.W. Gaeggeler, C. Boutron, U. Schotterer, L. Tobler, K.V. Van De Velde, C. Ferrari, G. Cozzi, K. Rosman and P. Cescon, *Post-17th-century changes of European lead emissions recorded in high-altitude alpine snow and ice*, Environmental Science & Technology **38** (4), 957-964 (2004).

[4] C. Girardet and C. Toubin, *Molecular atmospheric pollutant adsorption on ice: a theoretical survey*, Surface Science Reports **281**, 179 (2001).

[5] J.G. Dash, Haiying Fu and J.S. Wettlaufer, *The premelting of ice and its environmental consequences*, Rep. Prog. Phys. **58**, 115-167 (1995).

[6] A. Marcelli, G. Cibin, A. Raco *in progress*.

[7] S. Gunther, B. Kaulich, L. Gregoratti and M. Kiskinova, *Photoelectron microscopy and applications in surface and materials science*, Progress in Surface Science, Jul 2002.

[8] A. Marcelli, G. Cibin, *Il ghiaccio come materiale e matrice. Studio e caratterizzazione del ghiaccio, delle sue fasi, delle composizioni, dei contaminanti e del particolato mediante moderne tecniche spettroscopiche.* Collana dei Quaderni dell'INRM, n.**1** (2004).

7 APPENDIX

We report in detail the results of measurements of the different mechanical characteristics of the SpaceFab micromanipulator. The tests have been performed using a laser interferometer by ZLM Laser Meßtechnik in air.

7.1 Test of the static mechanical stability

To verify the system rigidity, the absence of vibrations and the stability for spectromicroscopy experiments, we measured the position of the manipulator head in static conditions, as a function of time. Data have been collected in air along the three orthogonal directions (X, Y, Z) . The changes in position, reported in the following plots, due to the possible presence of atmospheric turbulences and thermal variations in the interferometer beam path, allow the estimation of the upper limit for an effective movement of the manipulator head. The results show that, in the time range of 1 minute, the manipulator head can be considered stable, within a range of less than 80 nm.

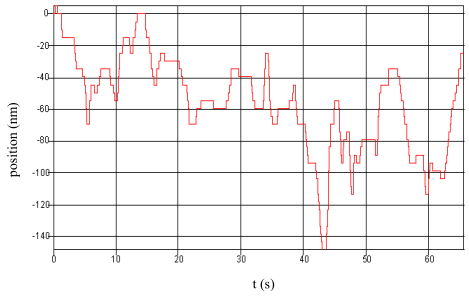

Head position vs. time along the X axis.

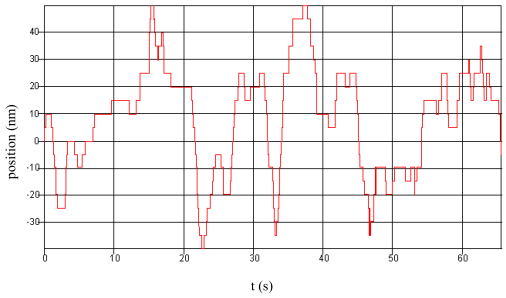

Head position vs. time along the Y axis.

Figure 6. Measured position of the micrometric head for about one minute in static conditions. The average movement is 20 nm, with a maximum displacement of 80 nm.

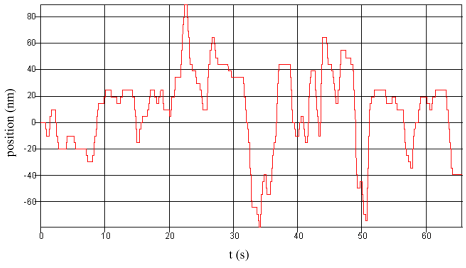

Head position vs. time along the Z axis.

7.2 Test of accuracy for translations (standard VDI/VE 2617)

The data show the positioning error of the measured translational motions of the manipulator head over the entire travel range (0-40 mm) along the X, Y, Z directions. The difference between a selected position and the achieved position is shown in each plot, together with the repeatability measurement. This latter value has been obtained through the repetition of the measurement and the calculation of the statistical standard deviation, reported as an error bar (dashed lines). The maximum position error is better than 10 μm for both X an Z axes while is about 50 μm for the Y axis. For all translational motions the repeatability is better than 1 μm.

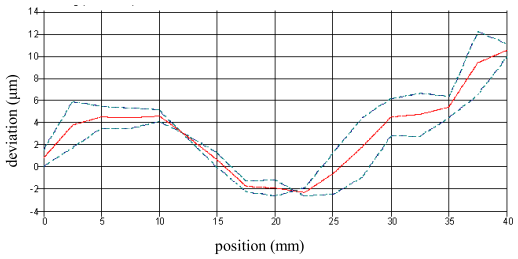

Positioning error for a motion along X axis.

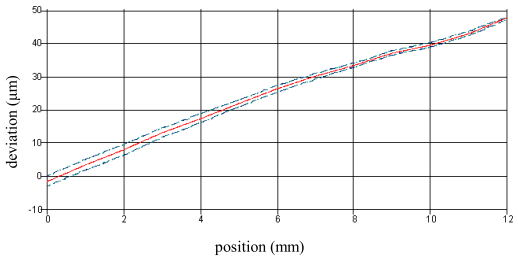

Positioning error for a motion along Y axis.

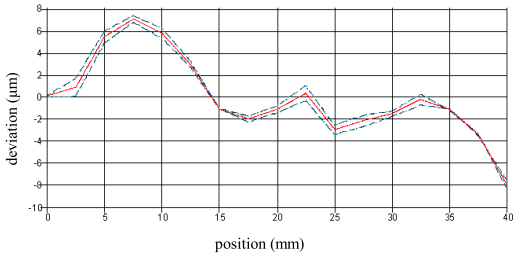

Positioning error for a motion along Z axis.

Figure 7: Results of the translation accuracy tests .

7.3 Test of transverse straightness

Here we report the set of measurements of the movement of the manipulator head in the transversal direction respect to a translation. To verify the motion regularity of the manipulator head, the perpendicular displacement (Y direction) is measured during X and Z motion. As before, the plots show the displacement vs. position and the statistical analysis with an error bar (dashed lines). The maximum measured displacement is less than 8 μm, while the reproducibility is better than 2 μm.

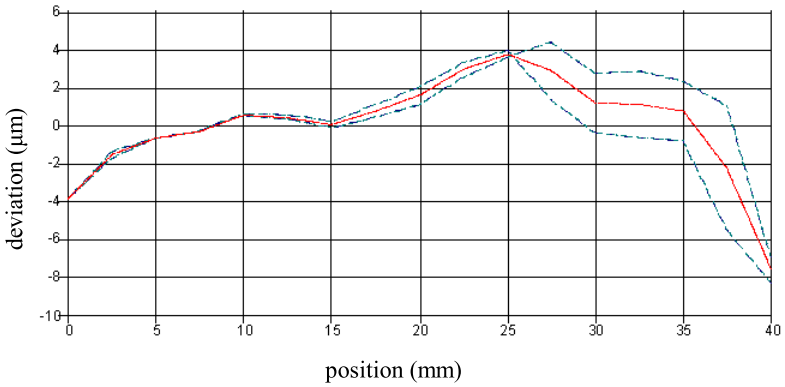

Height displacement vs. horizontal position (X axis).

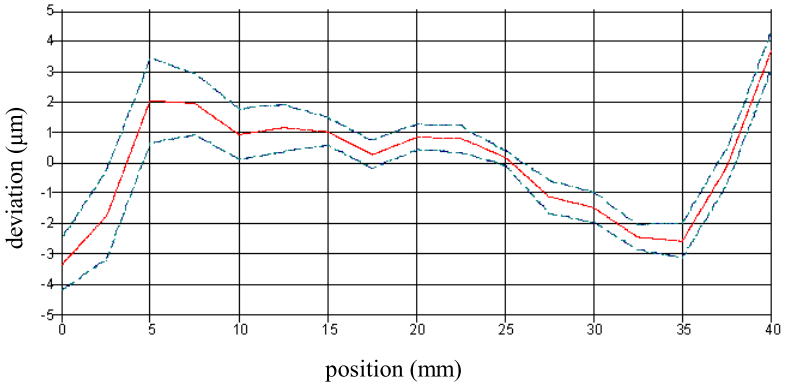

Height displacement vs. horizontal position (Z axis).

Figure 8: Results of the transverse straightness tests.

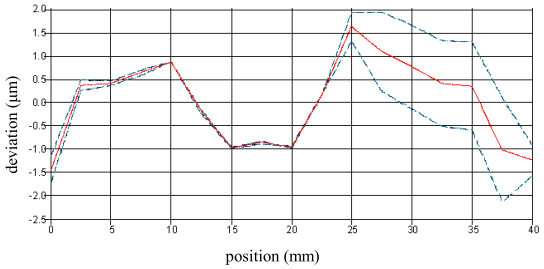

Measured transverse displacement (along Z axis) vs. horizontal position (X axis).

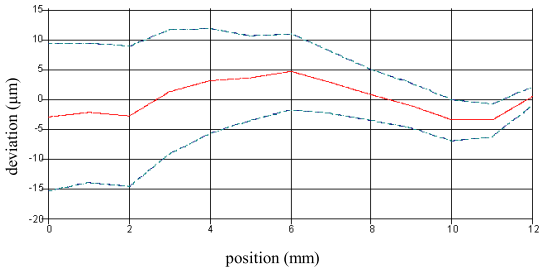

Measured transverse displacement (in the X, Z plane) vs. vertical position (Y axis).

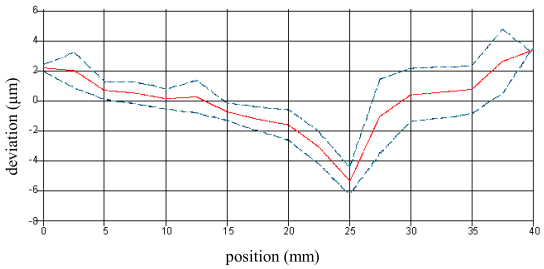

Measured transverse displacement (along X axis) vs. horizontal position (Z axis).

Figure 9: In the above plots are reported the transverse straightness tests in the horizontal plane (X, Z plane) for motions along the three axis (X,Y,Z).

7.4 Angular measurements

Tests were performed also to evaluate the displacement correlated to translational motions. The parallelism during translations of the head has been measured looking at the angular displacement in both vertical and horizontal planes.

7.4.1 Angular movements in the horizontal plane (pitch)

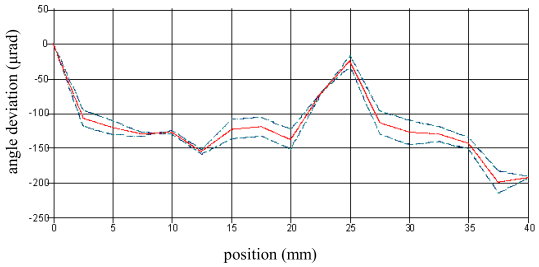

Measurement of the angular deviation of the head orientation in the horizontal plane (X,Z) vs. position, during a motion along X axis.

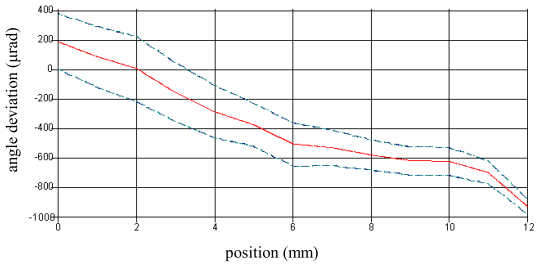

Measurement of the angular deviation of the head orientation in the horizontal plane (X,Z) vs. position during motion along Y axis.

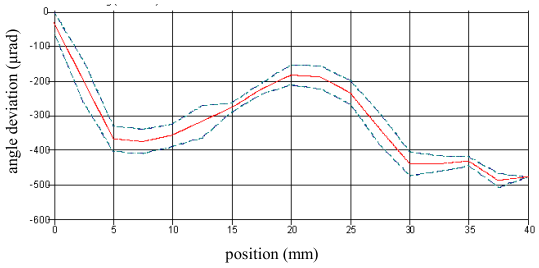

Measurement of the angular deviation of the head orientation in the horizontal plane (X,Z) vs. position during motion along Z axis.

Figure 10: The plots show the variation of the head direction during translations. The maximum angular displacement is better than 200 μrad.

7.4.2 Angular movements in the vertical plane (roll)

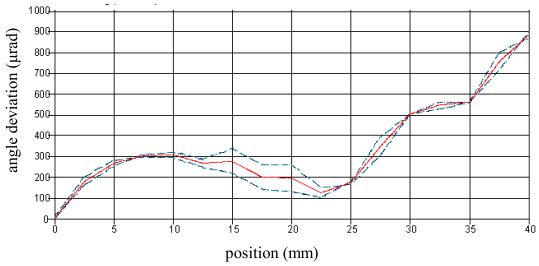

The angular deviation in the vertical plane vs. position during motion along X axis.

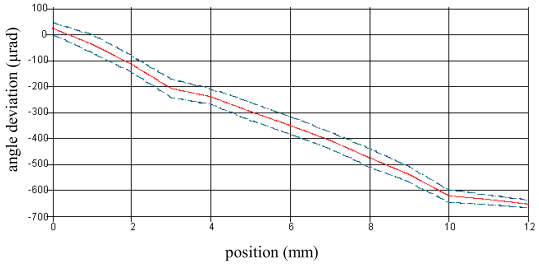

The angular deviation in the vertical plane vs. position during motion along Yaxis.

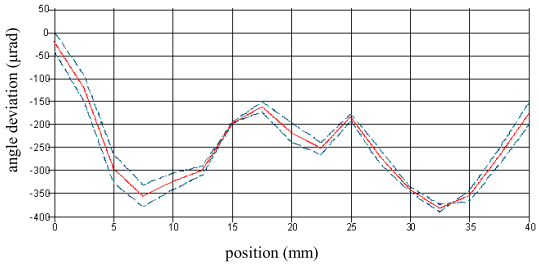

The angular deviation in the vertical plane vs. position during motion along Z axis.

Figure 11: The plots report the angular deviation of the micrometric head in the vertical plane during translations. The maximum displacement is better than 800 μrad, while the repeatability shown as error bars, is better than 100 μrad.

7.5 Accuracy tests for rotations

The rotation accuracy tests below reported have been performed for two different ranges: +/-4^o using angular steps of 0.5^o and +/-0.01^o with 0.001^o steps. These plots suggest a linear behavior as a function of the position of the related translational movement. The statistical error bars associated to rotations around X and Y axis are better than 50 μrad.

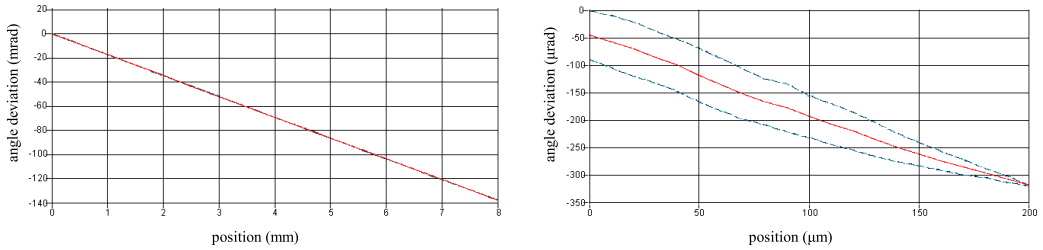

a) rotation angle vs. position for two angular ranges (140 mrad, 300μrad) around X axis.

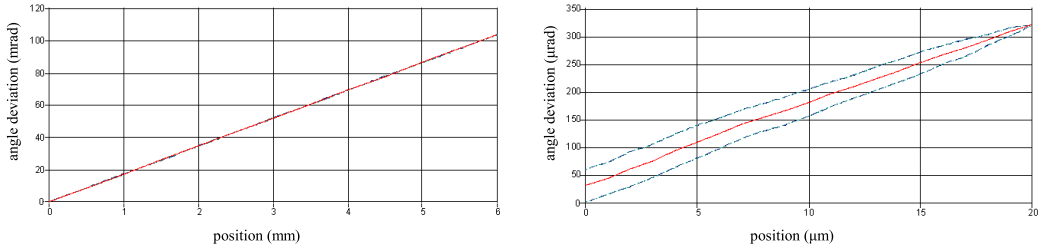

b) rotation angle vs. position for two angular ranges (120 mrad, 300μrad) around Y axis.

Figure 12: Accuracy tests for rotations around X and Y axes.

7.6 Tests of repeatability for translational and rotational step motions

7.6.1 Test of repeatability for translational step motions.

We measured the repeatability of the head position for motions along the X,Y,Z axes for both wide (0.1 mm) and small (0.1 μm) step motions. The measured position repeatability is better than 100 nm for a movement in a range of 700 nm.

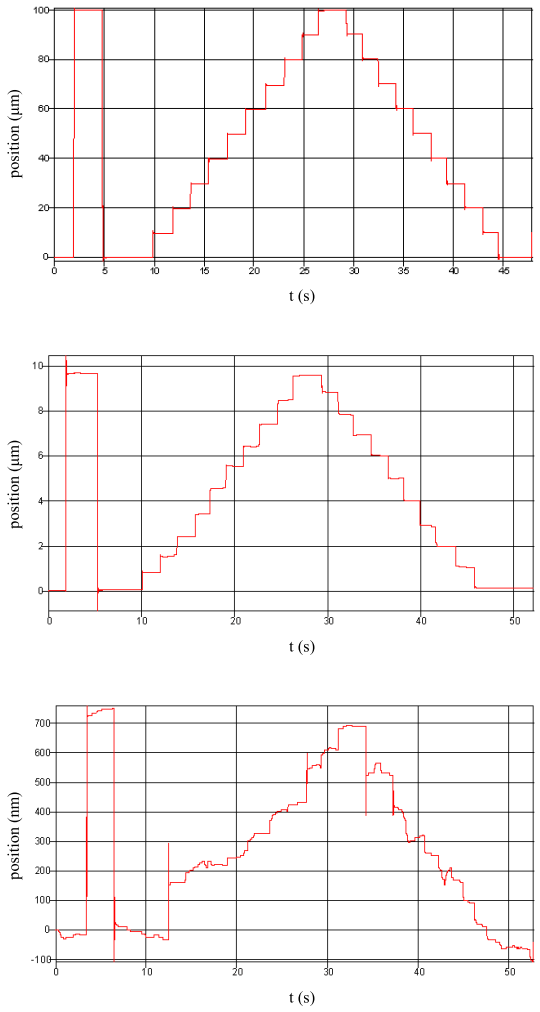

Figure 13: Position repeatability for a step motion cycles along the X direction. From top to bottom, the measured motion ranges were: 100, 10 and 0.7 μm.

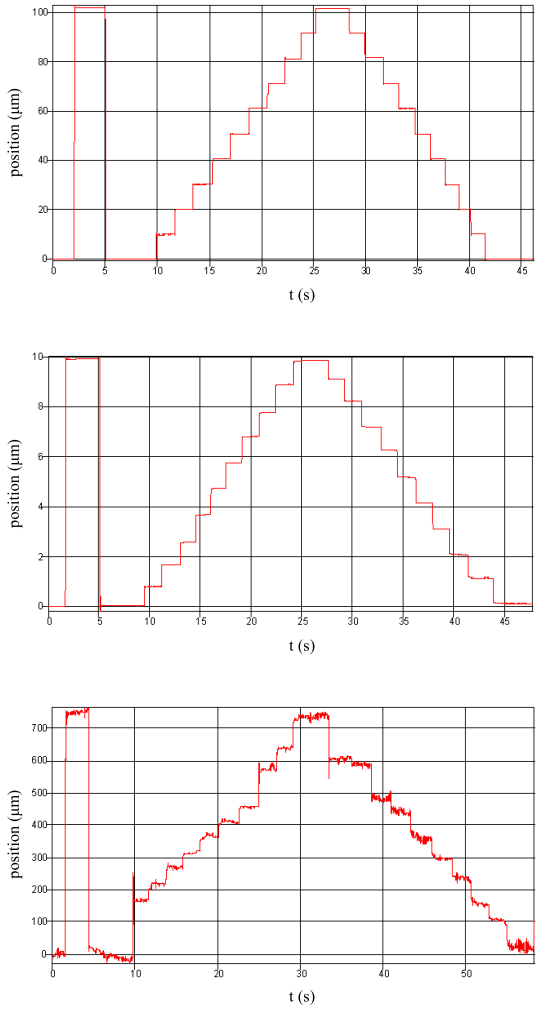

Figure 14: Position repeatability for a step motion cycles along the Y direction. From top to bottom, the measured motion ranges were: 100, 10 and 0.7 μm.

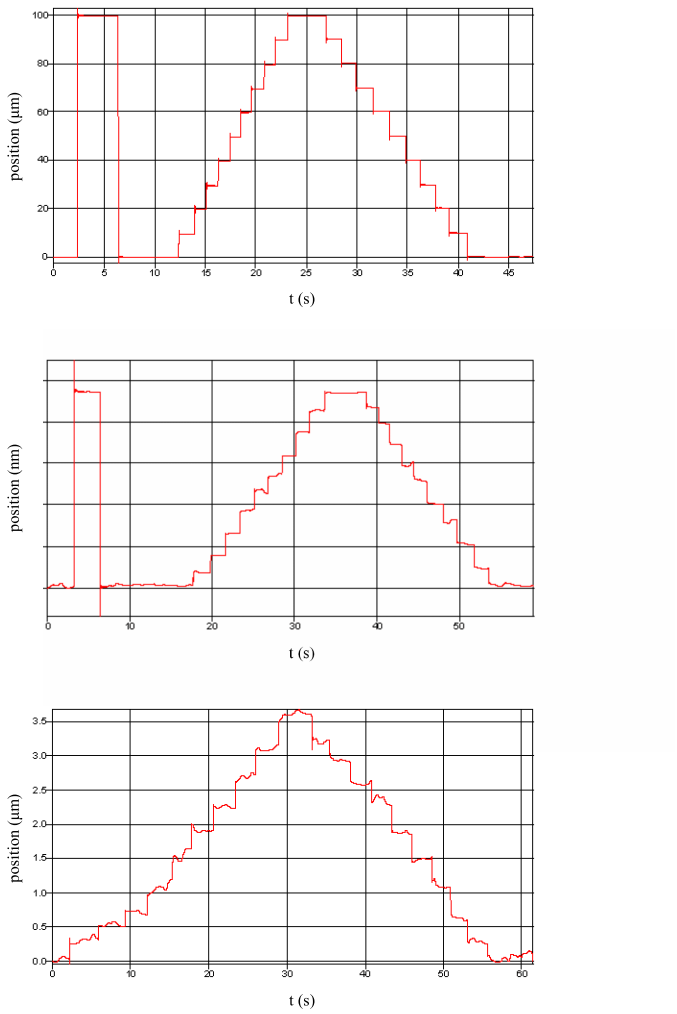

Figure 15: Position repeatability for a step motion cycles along the Z direction. From top to bottom, the measured motion ranges were: 100, 10 and 3.5 μm.

7.6.2 Test of repeatability for rotational step motions

We measured the repeatability of the motion of the head for rotations around the X,Y axes for both wide (16 mrad) and small (100 μrad) step motions. The observed position repeatability is better than 10 μrad.

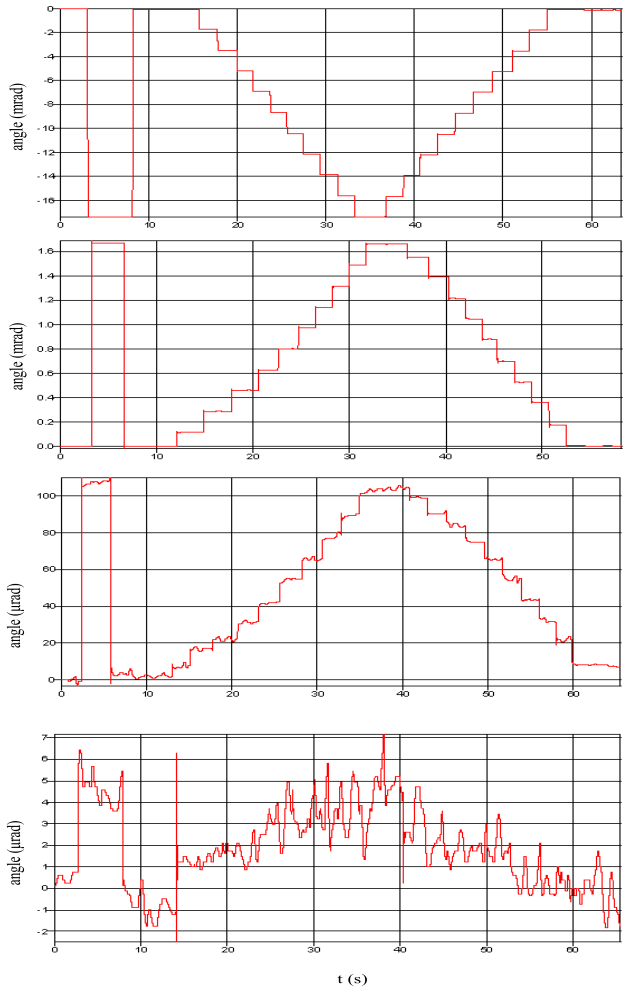

Figure 16: Position repeatability for a step rotation cycles around the X axis. From top to bottom, the measured motion ranges were: 16, 1.6 mrad, 100 and 6 μrad.

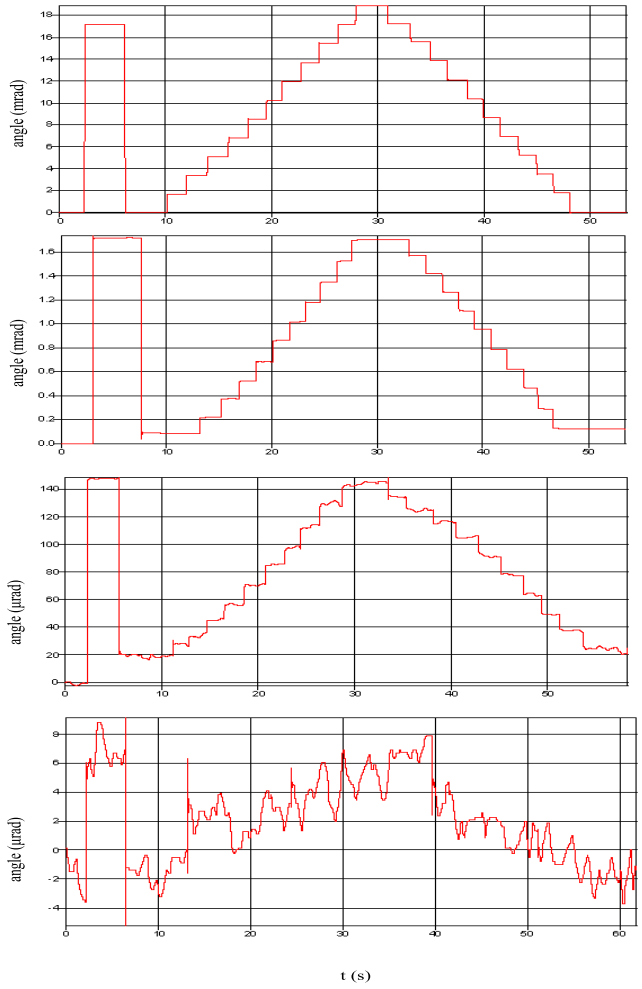

Figure 17: Position repeatability for a step rotation cycles around the Y axis. From top to bottom, the measured motion ranges were: 16, 1.6 mrad, 160 and 9 μrad.

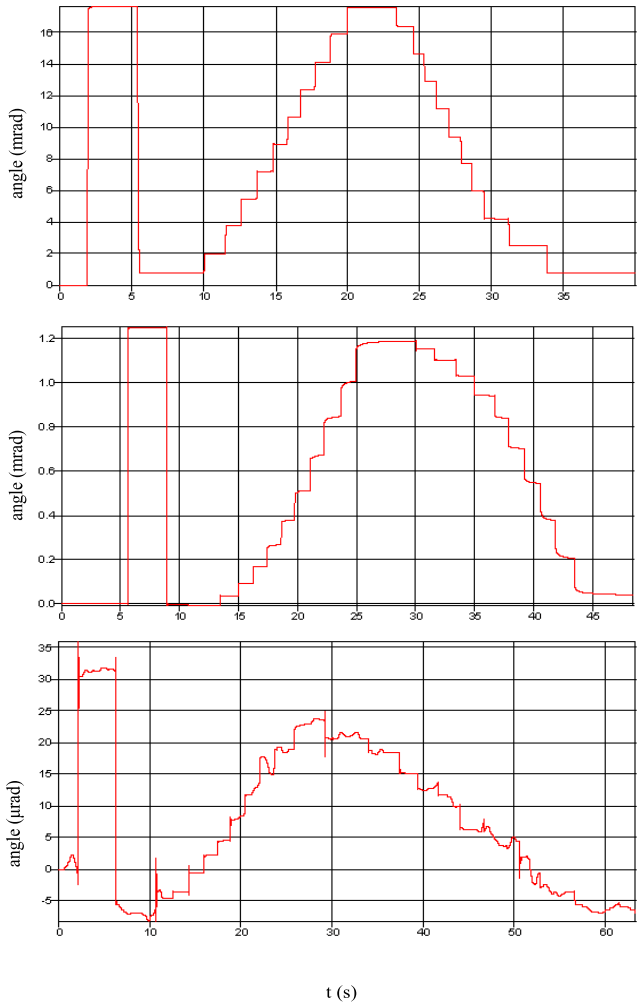

Figure 18: Position repeatability for a step rotation cycles around the Z axis. From top to bottom, the measured motion ranges were: 16, 1.6, 0.35 mrad.

7.7 Test of the dynamic stability of translations

The two plots report the measurement of the head position vs. time, during several step motion cycles performed with different resolutions. The data show the device stability during the motion, better than 0.2 μm during a translation step cycle of 10 μm of amplitude and for an observation time of a few seconds.

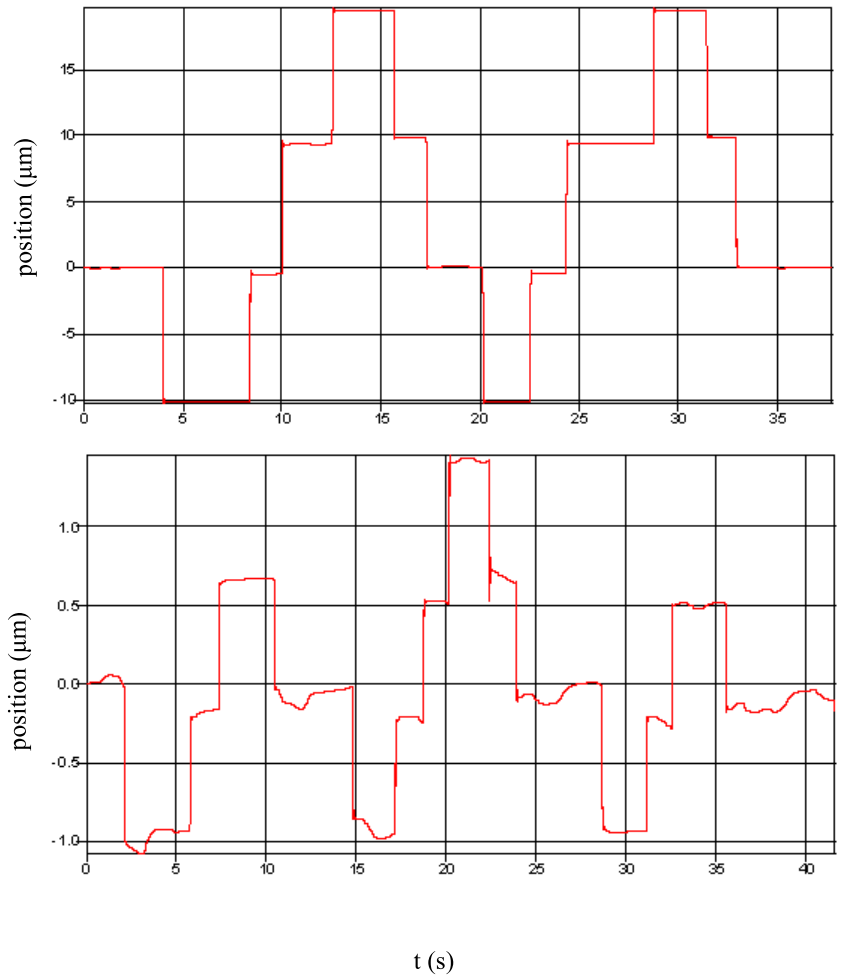

Figure 19: Dynamic stability test of the manipulator head. Top panel: step height 10 μm. Bottom panel: step height 1μm.